Intracavity laser spectroscopy of H_2O at 800 K

T.M. Petrova and L.N. Sinitsa

Institute of Atmospheric Optics,
Siberian Branch of the Russian Academy of Sciences, Tomsk

Received April 6, 2005

The absorption spectrum of water vapor in the region of 9387–9450 cm^{-1} is studied at a temperature of 800 K using an intracavity Nd-laser spectrometer. The high-temperature water vapor spectrum contains more than 150 absorption lines, 54% of which are assigned to 8 vibrational bands: $3\nu_2 + \nu_3$, $2\nu_1 + \nu_2$, $\nu_1 + \nu_2 + \nu_3$, $\nu_2 + 2\nu_3$, $2\nu_1 + \nu_3$, $3\nu_3 - \nu_2$, $\nu_1 + 2\nu_2 + \nu_3 - \nu_2$, $\nu_1 + 2\nu_3 - \nu_2$, $2\nu_1 + \nu_3 - \nu_2$.

The water molecule is one of the prevailing molecules in the Universe (it takes the third place after hydrogen and carbon monoxide). It plays an important role in atmospheric absorption of radiation and affects the radiation balance in the atmosphere. The water molecule is found in sunspots region and in many other space objects.

Information on water vapor spectroscopic characteristics is applicable in different scientific fields, e.g., flame physics, laser physics, manufacturing of ultra-pure materials.

Water vapor high-temperature spectra are studied comprehensively in microwave, far, and middle infrared ranges; and vibrational bands have been analyzed in the corresponding ranges.[1–7] The near infrared range above 9000 cm^{-1} remains practically uninvestigated because of small line intensity values. This range is of interest when studying the structure of high rotational levels of vibrational states, which form the second hexade of water vapor resonating states, in order to realize comprehensively the energy structure of molecules and to analyze the effect of intramolecular interactions on molecular spectra. Therefore, detailed experimental data on water vapor absorption spectra in the region above 9000 cm^{-1} is very important, especially at high temperatures. A high-sensitive spectral equipment is needed because of the low line intensity. One of the most sensitive spectroscopic techniques is intracavity (IC) laser spectroscopy with an absorption threshold sensitivity of 10^{-7}–10^{-9} cm^{-1}, which allows recording spectral regions up to 100 cm^{-1} in width during the generation pulse.

In this work, the water vapor absorption spectrum in the region of 1.06 μm at a temperature of 800 K is studied using the intracavity Nd-glass laser spectrometer.

Experiment

Figure 1 shows the block-diagram of the IC laser spectrometer based on an Nd-glass pulse laser.

The laser cavity, formed by spherical mirrors with high reflection coefficients within the 1.06 μm region, contains a heated optical cell with the analyzed substance. A special design of the cell allows measurements to be conducted at temperatures between 300 and 1000 K. Laser spectrum irregularity caused by "spurious" selection on optical scheme elements, recording system noises, and affecting the threshold sensitivity of the IC laser spectrometer, did not exceed 10%. Duration of laser generation, recorded with a photoresistor, was equal to 1 ms, which provided for registration of weak spectral lines with a minimal absorption coefficient of $5 \cdot 10^{-8}$ cm^{-1} at the signal-to-noise ratio equal to 10.

It is possible to observe spectral line displacements when recording temperature spectra, which are defined by spectral line shifts due to variations of the substance pressure and temperature, as well as adjustment of instruments. The interferometer, situated outside the laser cavity behind a 100% mirror, measured and recorded instrumental distortions. A typical pattern of combined radiation from laser and interferometer is shown in Fig. 2; the distance between minima is 0.22 cm^{-1}.

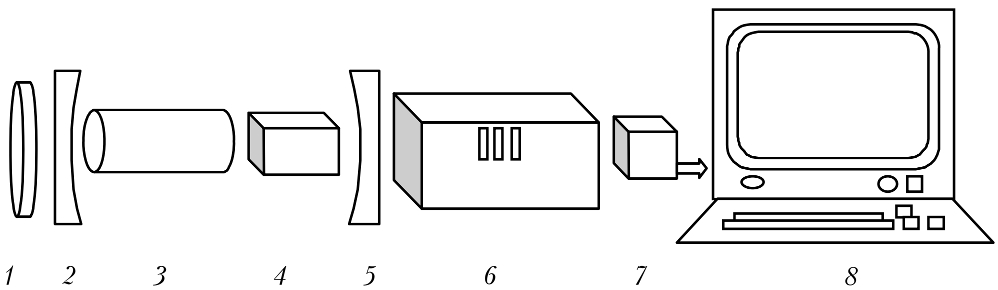

Fig. 1. Block-diagram of the experimental setup: interferometer (*1*), cavity mirrors (*2* and *5*), heated cell (*3*), active element (*4*), diffraction spectrograph DFS-8 (*6*), CCD photodetector (*7*), and PC (*8*).

0235-6880/05/09 723-06 $02.00

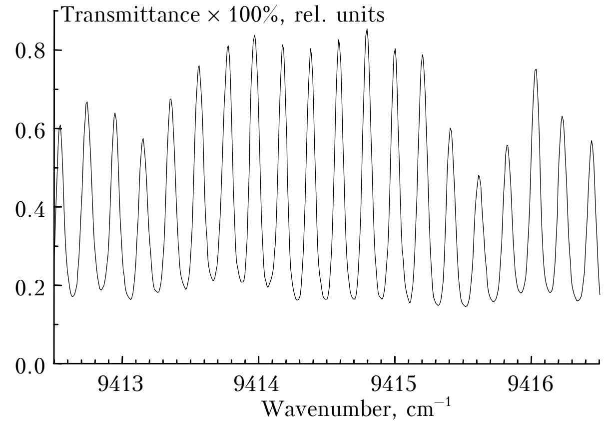

Fig. 2. A portion of spectrum of laser and interferometer combined radiation.

Spectra were recorded under overlapping of an external interferometer by a technique standard for IC spectroscopy. The DFS-8 diffraction spectrograph with a grating of 150 grooves/mm was used; it operated at a 1.06 μm wavelength in the 12th order. In this case, the spectral resolution, determined by the spectrograph, was equal to 0.03 cm^{-1}.

Analysis of the water vapor absorption spectrum

About 150 absorption lines of water vapor in 9387–9450 cm^{-1} region at a temperature of 800 K were detected. Lines, defined by transitions from vibrational levels greatly different in energy, were observed. Line intensities diversely varied with a temperature rise: lines with low-energy lower states weakened, while others with high-energy lower states manifested themselves in the spectrum. Lines from the first excited vibrational state (010) were detected. In this region, we detected only 50 lines at a temperature of 300 K, while at a temperature of 800 K the number of detected lines was considerably greater (about 150).

Due to water vapor pressure, absorption lines were broadened, and several lines manifested themselves under one profile (marked with # in Table 1). Three absorption lines centered at 9431.776, 9431.842, and 9431.911 cm^{-1} can exemplify the case. Two first lines were identified and referred to the (012) vibrational state (see Table 1).

The H_2O absorption spectrum in 9387–9450 cm^{-1} region was determined, first of all, by transitions to the second hexade of vibrational states. The strongest bands (111)–(000) and (012)–(000) are 300–400 cm^{-1} distant from the region under study (Fig. 3). Bands of the first decade of H_2O resonating state are centered far beyond the high frequency limit of the investigated range ((121)–(000) at 10328.72 cm^{-1} and (022)–(000) at 10521.7 cm^{-1}). Hence, in the indicated region, spectral lines with large rotational quantum numbers J and K are observed. Population of the (010) vibrational state increases several times, and hot bands, defined by transitions from the (010) state, appear in the spectrum. Such transitions are marked by circles in Fig. 3.

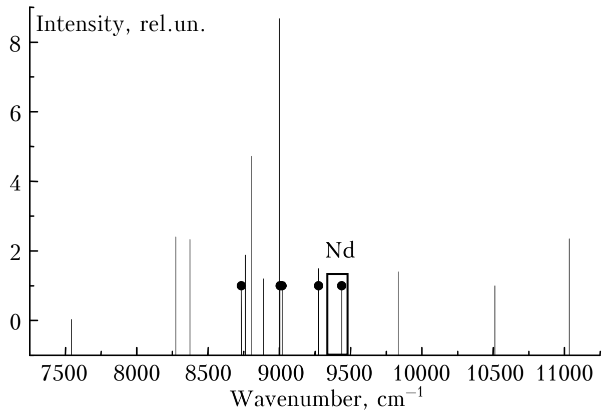

Fig. 3. Water vapor absorption bands in the range of Nd-glass laser radiation.

Interpretation of spectra is a very difficult problem, especially for C_{2v}-symmetry molecules. Due to comparative narrowness of the recorded spectrum, we could not use the combination difference method because of the absence of the necessary condition, namely, transitions to the same lower rotational levels. Therefore, for identification of spectral lines, we used a special program,[8] based on methods of the pattern recognition theory. The main parameters were:

– spectral line position;
– relative intensity of spectral line;
– tendency of spectral line center displacement from the calculated value.

Table 1

ν, cm^{-1}	Δν, cm^{-1}	$v_1'v_2'v_3'$	$v_1''v_2''v_3''$	$J'K_a'K_c'$	$J''K_a''K_c''$
1	2	3	4	5	6
9387.806	0.003				
9387.964	0.004	111	000	9 7 2	8 5 3
9388.753	0.003	111	000	9 7 3	8 5 4
9388.969	0.003	012	000	9 3 6	8 2 7
9389.396	0.003				
9389.560	0.007	012	000	10 4 6	9 3 7
9389.780	0.003				
9390.297*	0.003	031	000	9 6 4	8 2 7
9390.408	0.004				
9390.506	0.006	003	010	1 0 1	2 0 2
9391.380	0.006				
9391.513	0.004				

Table 1 (continued)

1	2	3	4	5	6
9391.995	0.005	012	000	8 8 1	7 7 0
		012	000	8 8 0	7 7 1
9392.511	0.004	012	000	9 7 2	8 6 3
		012	000	9 7 3	8 6 2
9393.027	0.004	201	010	12 4 8	11 2 9
9394.038	0.005				
9394.210	0.008				
9395.089*	0.004	031	000	13 5 8	12 1 11
9395.288	0.005				
9395.549	0.004				
9396.968	0.003	111	000	9 5 4	8 1 7
9397.070	0.004				
9398.321	0.005				
9398.543	0.007				
9398.699	0.008				
9399.214*	0.009	031	000	11 8 3	10 6 4
9399.415	0.008				
9399.558	0.005				
9399.708*	0.005	031	000	11 8 4	10 6 5
9399.820	0.004	111	000	13 5 9	12 3 10
9399.974	0.004				
9400.638	0.005				
9400.754	0.005				
9400.810	0.003				
9401.105	0.007				
9402.919	0.006				
9403.190	0.007	003	010	3 2 2	3 2 1
9403.966	0.009	111	000	12 2 10	11 0 11
9404.380	0.006	111	000	12 3 10	11 1 11
9404.879	0.004				
9404.987	0.003				
9405.154*	0.005	201	010	11 6 6	10 4 7
9405.465	0.009				
9405.796	0.003				
9405.999	0.004	210	000	13 2 11	12 1 12
9406.271	0.005				
9406.663 #	0.006				
9406.767 #	0.008	012	000	11 5 6	10 4 7
9407.267	0.005	111	000	10 7 3	9 5 4
9407.374	0.003	102	010	4 4 1	3 3 0
9407.547	0.005	012	000	4 4 0	3 3 1
9407.716	0.003	111	000	13 6 8	12 4 9
9408.144	0.003				
9409.125	0.003	012	000	8 3 6	7 0 7
9409.334*	0.006	121	010	14 3 11	13 1 12
9409.740 #	0.003	111	000	10 7 4	9 5 5
9409.860 #	0.006				
9410.455	0.005	210	000	9 6 3	8 3 6
9410.667 #	0.004	111	000	14 4 10	13 2 11
9410.802 #	0.005				
9411.024	0.003				
9411.416	0.003	012	000	9 8 2	8 7 1
		012	000	9 8 1	8 7 2
9411.688	0.004	102	010	8 8 1	7 7 0
		102	010	8 8 0	7 7 1
9412.412	0.005	012	000	10 7 4	9 6 3
9412.562	0.003	012	000	10 7 3	9 6 4
9412.784	0.004	012	000	8 4 5	7 1 6
9413.135*	0.005	031	000	16 7 10	15 5 11
9413.849	0.005	003	010	0 0 0	1 0 1
9414.270	0.003				
9415.880	0.004				
9416.189	0.005	210	000	14 4 11	13 1 12
9416.460	0.005	111	000	12 8 4	11 6 5
9417.330	0.005	102	010	5 5 0	4 4 1
9417.740	0.005	121	010	10 7 3	9 5 4
9417.923	0.008	111	000	12 8 5	11 6 6

Table 1 (continued)

1	2	3	4	5	6
9418.036	0.009				
9418.321	0.006	111	000	13 3 10	12 1 11
9418.479	0.01				
9418.650	0.006				
9418.782 #	0.004				
9418.853 #	0.01				
9419.164	0.01	102	010	7 7 1	6 6 0
		102	010	7 7 0	6 6 1
9419.290*	0.01	121	010	10 7 4	9 5 5
9420.079	0.003	111	000	13 4 10	12 2 11
9422.253 #	0.003				
9422.328 #	0.004				
9422.478 #	0.003				
9422.597 #	0.005				
9423.607	0.004	111	000	11 7 4	10 5 5
9423.865	0.003	111	000	8 8 1	7 6 2
		111	000	8 8 0	7 6 1
9424.180	0.01				
9424.980	0.005				
9425.270	0.006	003	010	1 1 1	1 1 0
9425.809	0.004	121	010	13 3 11	12 1 12
9425.926	0.009				
9426.083 #	0.008	121	010	10 5 5	9 1 8
9426.200 #	0.005				
9427.095 #	0.004				
9427.148 #	0.005				
9428.366	0.004	111	000	9 9 1	8 7 2
		111	000	9 9 0	8 7 1
9430.108 #	0.009	111	000	11 7 5	10 5 6
9430.391	0.005	012	000	10 8 3	9 7 2
		012	000	10 8 2	9 7 3
9430.852	0.007	111	000	13 8 5	12 6 6
9431.241	0.003	012	000	11 7 5	10 6 4
9431.776 #	0.006	012	000	9 9 0	8 8 1
		012	000	9 9 1	8 8 0
9431.842 #	0.006	012	000	11 7 4	10 6 5
9431.911 #	0.01				
9433.075	0.004	121	010	11 7 4	10 5 5
9434.322*	0.003	121	010	15 5 11	14 3 12
9434.452	0.009				
9434.568	0.007	111	000	13 8 6	12 6 7
9435.091	0.004	111	000	14 6 9	13 4 10
9435.368	0.004				
9435.902	0.008	012	000	12 6 7	11 5 6
9436.133	0.008	003	010	1 1 0	1 1 1
9436.527	0.004				
9437.109 #	0.005				
9437.191 #	0.005	121	010	11 7 5	10 5 6
9437.387	0.005	012	000	11 4 7	10 3 8
9437.654	0.003				
9439.383	0.003	111	000	13 7 7	12 5 8
9439.980	0.003				
9441.636	0.005	111	000	10 5 5	9 1 8
9441.723	0.01	102	010	8 7 2	7 6 1
9441.928	0.005	012	000	12 5 7	11 4 8
9442.121	0.005	111	000	14 8 6	13 6 7
9442.675	0.004				
9442.940	0.005				
9443.239 #	0.01	012	000	9 2 7	8 1 8
9443.294 #	0.006				
9444.884	0.009				
9445.213	0.007				
9445.444	0.006	012	000	10 3 7	9 2 8
9445.598	0.004				
9445.900	0.003				

Table 1 (continued)

1	2	3	4	5	6
9446.194	0.004				
9446.338	0.007	111	000	13 2 11	12 0 12
9446.608	0.005				
9446.781	0.005				
9447.493	0.01	111	000	9 8 2	8 6 3
		111	000	9 8 1	8 6 2
9447.865 #	0.01				
9447.965 #	0.007				
9448.586 #*	0.01	012	000	11 8 3	10 7 4
		012	000	11 8 4	10 7 3
9448.677 #*	0.01	012	000	9 4 6	8 1 7
9449.937 #	0.005				
9450.069 #	0.005				
9450.386	0.007	012	000	12 7 5	11 6 6
9450.584	0.005	012	000	12 6 6	11 5 7
9450.695	0.005	210	000	7 7 0	6 4 3
9450.935	0.07				
9451.030	0.10	111	000	10 9 2	9 7 3
		111	000	10 9 1	9 7 2
9451.210	0.01	111	000	13 3 11	12 1 12

As an initial approximation, we used the spectrum calculated with the "Spectroscopy of Atmospheric Gases" system, created at the Institute of Atmospheric Optics,[9] with the use of highly precise *ab initio* calculation for H_2O molecule[10] at a pressure of 40 Torr, temperature of 800 K, and path length of 10 km. Figure 4 shows fragments of calculated and recorded spectra; a good agreement between them is evident. Lines with the intensity greater than $1.5 \cdot 10^{-27}$ cm/mol are manifested themselves in the spectrum, that well agrees with the spectrometer threshold sensitivity.

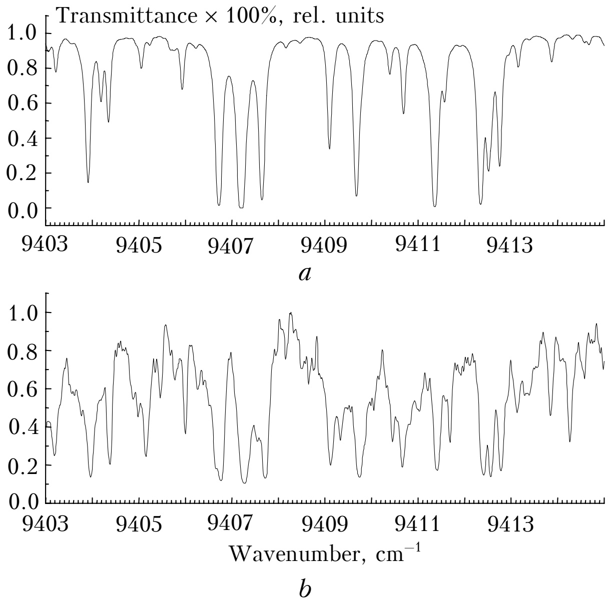

Fig. 4. Water vapor absorption spectrum in 9403–9415 cm^{-1} region: calculated with the use of Ref. 9 (*a*) and obtained in this work (*b*).

As a result of the study, 82 spectral lines of 152 water vapor absorption lines, recorded at a temperature of 800 K in the region of 9387–9450 cm^{-1}, were interpreted (see Table 1). The majority of lines was detected in (111)–(000) and (012)–(000) transitions. Calculated energy levels of vibrational states agreed with experimental ones in the limits of 0.02–0.07 cm^{-1}; as a rule, deviations were positive and remained almost the same for the same quantum number K_a at J changed. For levels with $J \leq 8$ and $K_a = 8$, a sharp change in regularities was observed, i.e., the value and the sign of deviations between experimental and calculated energy levels changed.

The (031)–(000), (121)–(010), and (201)–(010) bands are far distant from the spectral region under study. Though their spectral lines are of high intensity in the laser radiation range at a high temperature and have been identified by us, they need in additional experimental verification (in Table 1 they are marked by asterisks).

Lines assigned to eight rotational-vibrational transitions were identified. Five lines of $3\nu_2 + \nu_3$ band, 4 – of $2\nu_1 + \nu_2$, 32 – of $\nu_1 + \nu_2 + \nu_3$, 30 – of $\nu_2 + 2\nu_3$, and 4 – of the $2\nu_1 + \nu_3$ band were observed from the fundamental state.

Lines of hot rotational-vibrational transitions were also identified: 5 lines of $3\nu_3 - \nu_2$ band, 8 – of $\nu_1 + 2\nu_2 + \nu_3 - \nu_2$, 7 – of $\nu_1 + 2\nu_3 - \nu_2$, and 2 – of the $2\nu_1 + \nu_3 - \nu_2$ band.

About 46% of lines were not identified. In our opinion, they are defined by transitions to dark state levels or to levels with greater values of rotational quantum numbers and their predictive calculations are insufficiently precise.

Acknowledgments

This work was supported by the Russian Foundation for Basic Research (Grant No. 05–03–

32782), the Program of RAS "Optical spectroscopy and frequency standards," and INTAS (Grant No. 03–51–3394).

References

1. J.-M. Flaud, C. Camy-Peyret, and J.-P. Maillard, Mol. Phys. **32**, No. 2, 499–521 (1976).
2. C. Camy-Peyret, J.-M. Flaud, J.-P. Maillard, and G. Guelachvili, Mol. Phys. **33**, No. 6, 1641–1650 (1977).
3. R. Lanquetin, L.H. Coudert, and C. Camy-Peyret, J. Mol. Spectrosc. **206**, No. 1, 83–103 (2001).
4. R. Lanquetin, L.H. Coudert, and C. Camy-Peyret, J. Mol. Spectrosc. **195**, No. 1, 54–67 (1999).
5. N.F. Zobov, O.L. Polyansky, J. Tennyson, J.A. Lotosk, P. Colarusso, K.-Q. Zhang, and P.F. Bernath, J. Mol. Spectrosc. **193**, No. 1, 118–136 (1999).
6. O.L. Polyansky, N.F. Zobov, S. Viti, J. Tennyson, P.F. Bernath, and J. Wallace, J. Mol. Spectrosc. **186**, No. 2, 442–447 (1997).
7. http://www.tampa.phys.ucl.ac.uk/jonny/.
8. A.P. Shcherbakov, Atmos. Oceanic Opt. **10**, No. 8, 591–597 (1997).
9. http://spectra.iao.ru.
10. H. Partridge and D.W. Schwenke, J. Chem. Phys. **106**, No. 11, 4618–4639 (1997).